

## Impact of Muon Anomalous Magnetic Moment on Supersymmetric Models

Howard Baer<sup>1</sup>, Csaba Balázs<sup>2</sup>, Javier Ferrandis<sup>3</sup> and Xerxes Tata<sup>2</sup>

<sup>1</sup>*Department of Physics, Florida State University, Tallahassee, FL 32306 USA*

<sup>2</sup>*Department of Physics and Astronomy, University of Hawaii, Honolulu, HI 96822, USA*

<sup>3</sup>*Instituto de Física Corpuscular – C.S.I.C. – Universitat de València*

*Ed. de Institutos de Paterna – Apartado de Correos 22085 - 46071 València, Spain*

(February 8, 2020)

### Abstract

The recent measurement of  $a_\mu = \frac{g_\mu - 2}{2}$  by the E821 Collaboration at Brookhaven deviates from the quoted Standard Model (SM) central value prediction by  $2.6\sigma$ . The difference between SM theory and experiment may be easily accounted for in a variety of particle physics models employing weak scale supersymmetry (SUSY). Other supersymmetric models are distinctly disfavored. We evaluate  $a_\mu$  for various supersymmetric models, including minimal supergravity (mSUGRA), Yukawa unified  $SO(10)$  SUSY GUTs, models with inverted mass hierarchies (IMH), models with non-universal gaugino masses, gauge mediated SUSY breaking models (GMSB), anomaly-mediated SUSY breaking models (AMSB) and models with gaugino mediated SUSY breaking (inoMSB). Models with Yukawa coupling unification or multi-TeV first and second generation scalars are disfavored by the  $a_\mu$  measurement.

PACS numbers: 14.80.Ly, 13.40.Em, 12.60.Jv

## I. INTRODUCTION

Recently, the Brookhaven E821 experiment has announced a new measurement of the anomalous magnetic moment of the muon [1]. The measured result deviates by  $2.6\sigma$  from the central value of the quoted Standard Model (SM) prediction [2]:  $a_\mu(exp) - a_\mu(SM) = 43(16) \times 10^{-10}$ , where  $a_\mu = \frac{g_\mu - 2}{2}$ . The largest error on the SM calculation arises from the hadronic vacuum polarization loops. These loops are included via dispersion integrals involving the rate for  $e^+e^- \rightarrow hadrons$ , with the largest contribution coming from the region around the  $\rho(770)$  resonance. We note that different evaluations<sup>1</sup> of the hadronic vacuum polarization contribution can lead to a SM  $a_\mu$  prediction in accord with experiment: see Ref. [4]. It is anticipated that improved measurements of these low energy cross section measurements will reduce the uncertainty in the SM prediction in the near future, without recourse to tau decay data. Furthermore, additional data already taken by the E821 collaboration should soon reduce the experimental uncertainty in  $a_\mu$  by about a factor of two. If the difference between SM prediction and experimental measurement of  $a_\mu$  is maintained and sharpened, then a clear signal for physics beyond the SM will be obtained.

The error bars on  $a_\mu$  are now small enough to be sensitive to electroweak loop effects, and other effects of the same order of magnitude. Weak scale supersymmetry is an especially well motivated extension of the SM in which contributions to  $a_\mu$  from loops with supersymmetric (SUSY) particles naturally have a magnitude comparable to electroweak effects. Thus the Brookhaven experiment can potentially probe weak scale supersymmetry. Supersymmetric contributions to  $a_\mu$  have been calculated previously [5,6], including a number of very recent papers addressing the new E821 result [7–18]. The supersymmetric contributions to  $a_\mu$  involve chargino-sneutrino loops and also neutralino-smuon loops. For  $\tan\beta \equiv \frac{v_u}{v_d}$  not too small, the supersymmetric contributions yield [6]

$$\Delta a_\mu^{SUSY} \propto \frac{m_\mu^2 \mu M_i \tan\beta}{M_{SUSY}^4}, \quad (1.1)$$

where  $M_i$  ( $i = 1, 2$ ) is a gaugino mass, and  $M_{SUSY}$  is a characteristic sparticle mass scale. Then  $\Delta a_\mu^{SUSY}$  grows with  $\tan\beta$ , and has the same sign as the superpotential Higgs mass term  $\mu$ .

In this paper, we present calculations of the contribution to  $a_\mu$  from a variety of supersymmetric models. Some of these models overlap with those recently examined in Ref. [8,10,11,13,16], while others are new. In addition, we compare explicitly where possible with reach projections of Run 2 of the Fermilab Tevatron  $p\bar{p}$  collider and the CERN Large Hadron Collider (LHC).

The supersymmetric models considered can be organized according to the assumed mechanism for communication of supersymmetry breaking from the hidden sector to the visible

---

<sup>1</sup>The evaluation by Davier and Höcker [3] uses the much more precise tau decay data to reduce the uncertainty in the  $e^+e^- \rightarrow \pi^+\pi^-$  cross section. This is a potential source of theoretical uncertainty since the tau decays purely via the weak isospin 1 channel, while the photon also has an isospin zero component.

sector. First, we consider models with SUSY breaking communicated via gravitational interactions. These include the minimal supergravity model (mSUGRA), with universality of soft SUSY breaking terms at the Grand Unification Theory (GUT) scale. In addition, we also consider minimal  $SO(10)$  models with a high degree of Yukawa coupling unification [19], models with an inverted scalar mass hierarchy (proposed to solve the SUSY flavor and CP problems), and models with non-universal gaugino masses. Next, we show results for models with gauge-mediated SUSY breaking (GMSB), for various numbers of messenger fields. We also examine models with anomaly-mediated SUSY breaking (AMSB) and finally, models with gaugino-mediated SUSY breaking (inoMSB). We end with some broad conclusions in the last section. If the apparent discrepancy between theory and experiment continues to hold, then SUSY GUT models with a high degree of Yukawa unification will be strongly constrained, as will be models which solve the SUSY flavor and CP problems via a decoupling of the first two generations of scalars.

## II. GRAVITY-MEDIATED SUSY BREAKING MODELS

In this class of models, SUSY is assumed to be broken in a hidden sector, consisting of fields which do not interact with usual particles and their superpartners via SM gauge or Yukawa type interactions. SUSY breaking is communicated to the visible sector via gravitational interactions. In general, there is no mechanism to suppress soft SUSY breaking terms which can lead to flavor changing (FC) and CP violating processes in conflict with experiment. A common (ad-hoc) solution is to assume *universality* of soft SUSY breaking terms at the unification scale, which suppresses the unwanted FC processes.

### A. Minimal supergravity model (mSUGRA)

In this model [20], it is assumed that, at the GUT scale, all scalars have a common mass  $m_0$ , all gauginos have a common mass  $m_{1/2}$ , and all trilinear soft SUSY breaking terms have a common value  $A_0$ . Electroweak symmetry is assumed to be broken radiatively (REWSB), leading to a model parameter set consisting of

$$m_0, m_{1/2}, A_0, \tan\beta, \text{sign}(\mu). \quad (2.1)$$

The superparticle masses and mixings can be calculated via renormalization group evolution between the scale of grand unification and the weak scale. We use the mSUGRA mass calculation embedded in the computer program ISAJET 7.51 for our results [21]. We have adapted the  $\Delta a_\mu^{SUSY}$  calculation of Moroi [6] for use with the ISAJET code.

Our results for the mSUGRA model are shown in Fig. 1. We plot only parameter planes with  $\mu > 0$ , since the opposite sign of  $\mu$  almost always gives negative contributions to  $\Delta a_\mu^{SUSY}$ . The solid shaded regions are excluded by *i*) a lack of appropriate REWSB, or *ii*) a lightest SUSY particle that is not the lightest neutralino ( $\tilde{Z}_1$ ), or *iii*) by the experimental lower limits from LEP2 that  $m_{\tilde{W}_1} > 100$  GeV,  $m_{\tilde{e}_1} > 100$  GeV and  $m_{\tilde{\tau}_1} > 76$  GeV. The region below the thick solid contour has a lightest Higgs mass  $m_h < 113.5$  GeV, in apparent discord with recent results [22] from LEP2 on searches for SM Higgs bosons. The dots shaded regions are found to have a value of  $\Delta a_\mu^{SUSY}$  within  $2\sigma$  of the E821 result: *e.g.*

$11 \times 10^{-10} < \Delta a_\mu^{SUSY} < 75 \times 10^{-10}$ . The regions below the dashed contours are accessible to SUSY searches via the isolated trilepton or  $\cancel{E}_T$  signals at Run 2 of the Tevatron with  $25 \text{ fb}^{-1}$  of integrated luminosity [23,24]. Finally, the region below the dot-dashed contour is accessible to SUSY searches at the CERN LHC  $pp$  collider, assuming  $10 \text{ fb}^{-1}$  of integrated luminosity [25].

In Fig. 1a), we show the  $m_0$  vs.  $m_{1/2}$  plane for  $\tan \beta = 3$ , and for  $A_0 = -2m_0$ . For larger values of  $A_0$ , we find the entire plane to be excluded<sup>2</sup> by LEP2 Higgs searches. At this low value of  $\tan \beta$ , the region preferred by the E821 result consists of a small region in the lower left corner. The preferred region lies entirely within the Tevatron Run 2 search region, but is unfortunately already disfavoured by LEP2 Higgs searches. In frame b), we show the same plane, but for  $\tan \beta = 10$  and  $A_0 = 0$ . In this case, the LEP2 Higgs bound cuts out a significant portion of the region preferred by  $\Delta a_\mu^{SUSY}$ , but a substantial region remains at low  $m_0$  where  $m_h > 113.5 \text{ GeV}$ . Much of this region is beyond the reach of Tevatron Run 2 experiments, but all of the preferred region is well within the region accessible to LHC searches. Of particular interest is that models with large  $m_0$  and low  $m_{1/2}$ , *i.e.* in the focus point region [26], are disfavored, and will be excluded if the disagreement between theory and experiment persists. Finally, in frame c), we show the same parameter space plane as in b), except now for  $\tan \beta = 35$ . The region preferred by  $\Delta a_\mu^{SUSY}$  has expanded greatly, reflecting the nearly linear growth of  $\Delta a_\mu^{SUSY}$  with  $\tan \beta$ . Much of the region is beyond the LEP2 Higgs bound, but all of it is within the reach of the CERN LHC. In this case, the focus point region *is* allowed for large  $\tan \beta$ .

In several papers, comparisons have been made between the calculated values of  $\Delta a_\mu^{SUSY}$  and the  $b \rightarrow s\gamma$  decay rate, and the neutralino relic density  $\Omega_{\tilde{Z}_1} h^2$ . It is especially interesting to note that at large  $\tan \beta$  and  $\mu < 0$ , the mSUGRA model is doubly disfavored by both  $\Delta a_\mu^{SUSY}$  and by  $b \rightarrow s\gamma$  [27]. In addition, at large  $\tan \beta$ , much of mSUGRA model parameter space at large values of  $m_0$  and  $m_{1/2}$  is allowed by bounds on the neutralino relic density [28–30]. This is due in large part to  $\tilde{Z}_1 \tilde{Z}_1 \rightarrow A, H \rightarrow b\bar{b}$  annihilation via very broad  $A$  and  $H$  poles in the  $s$ -channel. It is an important observation that the mSUGRA model can accommodate all these constraints, and simultaneously respect the bound from LEP2 Higgs searches.

## B. Yukawa unified $SO(10)$ model

Supersymmetric  $SO(10)$  grand unified models are especially attractive in that they can unify gauge couplings, Yukawa couplings and also matter particles within a single generation. In light of evidence for neutrino mass from observation of atmospheric neutrinos [31], there has been heightened interest in this class of models [32].  $SO(10)$  SUSY GUT models

---

<sup>2</sup>Strictly speaking, the bound  $m_h > 113.5 \text{ GeV}$  applies to the SM Higgs boson and needs to be corrected for the SUSY case. However, over much of the parameter space  $h$  is close to the SM Higgs boson, and we will for simplicity use this as the limit in the rest of this paper. For this reason, as well as to allow for some uncertainty in the computation of  $m_h$ , the reader should allow some latitude in the interpretation of this contour.

naturally accommodate light neutrinos via the see-saw mechanism. Using third generation fermion masses as inputs, Yukawa unification can be achieved if  $\tan\beta \sim 50$  and  $\mu < 0$ . In this region of parameter space, however, REWSB is not possible assuming universal scalar masses at the GUT scale. Incorporation of  $D$ -term scalar mass contributions, which are generically present when  $SO(10)$  breaks to a lower rank gauge group, allow REWSB to occur by imposing GUT scale boundary conditions where  $m_{H_u} < m_{H_d}$  [33]. In this case, the  $D$ -terms leave a characteristic imprint on the entire SUSY particle mass spectrum. The model parameter space consists of

$$m_{16}, m_{10}, M_D^2, m_{1/2}, A_0, \tan\beta, \text{ and } \text{sign}(\mu). \quad (2.2)$$

Here,  $m_{16}$  is the common soft SUSY breaking mass (renormalized at the GUT scale) of all matter scalars, while  $m_{10}$  is the corresponding mass of the Higgs scalars.  $M_D$  parametrizes the magnitude of the  $SO(10)$   $D$ -terms. Yukawa coupling unification restricts  $\tan\beta \sim 50 \pm 4$  and  $\mu < 0$ . The sparticle mass spectrum, relic density,  $b \rightarrow s\gamma$  decay rate, and collider signals have been recently calculated in terms of these parameters in the second paper of Ref. [33].

One might expect these models to be heavily disfavored by the E821 result, since Yukawa unification occurs for  $\mu < 0$ , while a positive value of  $\Delta a_\mu^{SUSY}$  occurs for  $\mu > 0$ . We explicitly display these results in Fig. 2, for *a*)  $\tan\beta = 47$  and *b*)  $\tan\beta = 50$ . We generate models with values of  $m_{16}$  and  $m_{10}$  over the range 0–3000 GeV,  $m_{1/2} : 0–1000$  GeV,  $-3000 < A_0 < 3000$  GeV and  $M_D < 1000$  GeV, and accept models that satisfy REWSB and phenomenological constraints, as well as having  $t - b - \tau$  Yukawa coupling unification at  $M_{GUT}$  to 5%. In both frames, we see that  $\Delta a_\mu^{SUSY}$  is always less than zero. However, for  $\tan\beta = 47$ , a substantial fraction of models have  $|\Delta a_\mu^{SUSY}| < 5$ , so that they lie within  $3\sigma$  of the E821 result. These models generally require  $m_{16} > 1000$  GeV, so are effectively entering the decoupling regime. In frame *b*), for  $\tan\beta = 50$ , almost all models are excluded unless  $m_{16} > 2200$  GeV. For the higher  $\tan\beta$  value, larger values of  $M_2$  and smaller values of  $|\mu|$  are generated for Yukawa unified solutions; in some cases, neutralino loops dominate the amplitude for  $\Delta a_\mu^{SUSY}$ . Overall, for  $\tan\beta = 50$ , there is decoupling at larger values of  $m_{16}$  than in the  $\tan\beta = 47$  case. In these models, generally a reasonable value for  $\Omega_{\tilde{Z}_1} h^2$  can be obtained [33]. Also, in these decoupling regimes, the rate for anomalous supersymmetric contributions to  $b \rightarrow s\gamma$  decay rate also diminishes. However, such large values of  $m_{16}$  may suffer from problems with naturalness.

### C. Inverted scalar mass hierarchy models

A possible solution to the SUSY flavor and CP problems arises by *decoupling* the matter scalars in the theory. This involves setting matter scalar masses towards the 10-100 TeV range, thereby suppressing all loop induced FCNCs and CP violating processes [34]. Such models seemingly violate constraints from naturalness, but two ways out have been suggested. In the focus point region of mSUGRA models [26], large  $m_0$ , small  $m_{1/2}$  and moderate to large  $\tan\beta$  yields a small value for  $|\mu|$  and possibly a small fine tuning of model parameters to achieve REWSB. An alternative is in models with an inverted scalar mass hierarchy (IMH), wherein first and second generations have multi-TeV masses, while third

generation scalars have sub-TeV masses: this latter condition results in models satisfying “naturalness”, since third generation scalar masses enter the fine-tuning calculation, while first and second generation masses are most severely constrained by flavor and CP violating processes.

### 1. Radiatively driven IMH model

An intriguing scenario has been proposed in Ref. [35], wherein the IMH is generated *radiatively* by starting with multi-TeV masses for *all* scalars at the GUT scale. At large  $\tan\beta$ , and for special soft SUSY breaking boundary conditions, third generation scalar masses are driven to weak scale values via renormalization group evolution, while first and second generation scalars remain at multi-TeV values, owing to their small Yukawa couplings. The proposed model incorporates  $t - b - \tau$  Yukawa coupling unification, and necessarily includes right neutrino superfields (as in  $SO(10)$ ), and requires the special ( $SO(10)$  symmetric) boundary conditions  $A_0^2 = 2m_{10}^2 = 4m_{16}^2$  for the renormalization group evolution of the soft SUSY breaking parameters. For consistency of Yukawa coupling unification with REWSB,  $SO(10)$   $D$ -terms are again necessary [36]. Thus, the parameter space of the RIMH model consists of

$$m_{16}, m_{1/2}, \tan\beta, M_D^2, M_N, \text{ and } \text{sign}(\mu). \quad (2.3)$$

The value of  $\tan\beta$  is generally large to achieve Yukawa unification, and the parameter  $M_N$  is the scale of the superpotential singlet neutrino mass term:  $10^3 \text{ TeV} < M_N < M_{GUT}$ , with  $M_N \sim 10^{15} \text{ GeV}$  favored by data from atmospheric neutrinos in the simplest seesaw model for neutrino masses. Only a modest IMH is possible. The mass spectra associated with these models, along with expectations for relic density,  $b \rightarrow s\gamma$  decay rates and collider signals, have been discussed in Ref. [36,37].

Motivated by the considerations in Ref. [37], we show in Fig. 3a) the masses of several sparticles, and in b) the associated value of  $\Delta a_\mu^{SUSY}$ , for  $\mu < 0$ ,  $\tan\beta = 50$ ,  $M_D = 0.2m_{16}$ ,  $m_{1/2} = 0.25m_{16}$  and  $M_N = 1 \times 10^7 \text{ GeV}$ . These parameters give a reasonable IMH while maintaining a calculable sparticle mass spectrum. In a), the IMH is displayed by the mass gap between  $m_{\tilde{\mu}_1}$  and  $m_{\tilde{t}_1}$  and  $m_{\tilde{b}_1}$ . In b), we see that  $\Delta a_\mu^{SUSY}$  is always negative for this case. However, for values of  $m_{16} > 3000 \text{ GeV}$ , the value of  $\Delta a_\mu^{SUSY}$  is within  $3\sigma$  of the E821 result, as the model moves into the decoupling regime. Such large values of  $m_{16}$  appear to be beyond the reach of even the LHC, at least for an integrated luminosity of  $10 \text{ fb}^{-1}$  [37].

We have also examined the situation regarding  $a_\mu$  for  $\mu > 0$ . In this case, as discussed in Ref. [37] Yukawa couplings do not unify well, and the unification parameter  $R$  typically ranges between 1.6 and 1.9. Here, we have fixed  $M_D = 0.2m_{16}$  which tends to give the largest mass hierarchy [37] for the chosen  $\tan\beta = 50$ . The results of our analysis are shown in Fig. 4 for a)  $M_N = 10^7 \text{ GeV}$ , and b)  $M_N = 10^{15} \text{ GeV}$ . The shaded regions are excluded because there is no REWSB, or one of the scalar mass parameters is tachyonic, or the lightest supersymmetric particle (LSP) is not a neutralino. To the right of the solid line, the crunch factor  $S$  defined in Ref. [37] exceeds 4. The dotted area shows the  $2\sigma$  region preferred by the result of E821 experiment.

In Fig. 5, we show  $\Delta a_\mu^{SUSY}$  versus  $m_{16}$  for the slice of Fig. 4a with  $m_{1/2} = 0.22m_{16}$  for which the hierarchy tends to be large. We see that  $\Delta a_\mu^{SUSY}$  is within  $2\sigma$  of the E821

central value when  $m_{16} < 1700$  GeV. SUSY signals should readily be observable throughout this range, which unfortunately is disfavoured by considerations of relic density and the branching ratio for the  $b \rightarrow s\gamma$  decay [37].

## 2. GUT scale IMH model

In this class of models, it is assumed the IMH already exists at the GUT scale. The model parameter space is

$$m_0(1), m_0(3), m_{1/2}, A_0, \tan\beta \text{ and } \text{sign}(\mu), \quad (2.4)$$

where  $m_0(1)$  is the common mass of first and second generation scalars at  $M_{GUT}$ , while  $m_0(3)$  is the mass of all third generation and Higgs scalars at  $M_{GUT}$ . In this case, two-loop contributions from first and second generation scalars to RG evolution of third generation scalars helps to drive the latter to small masses; to avoid tachyons,  $m_{1/2}$  must be chosen large enough. These models have been recently explored in Ref. [38,39]. In general, GUT scale IMH models can support much larger first and second generation scalar masses than RIMH models. This helps to further suppress FC and CP violating processes, but will also suppress anomalous contributions to  $a_\mu$ . For instance, for the two case studies presented in Table 1 of Ref. [39], we find  $\Delta a_\mu^{SUSY} = 1.6 \times 10^{-13}$  (case 1) and  $1.8 \times 10^{-11}$  (case 2). Hence, these models should give  $a_\mu$  values very close to the SM prediction.

## D. $SU(5)$ models with non-universal gaugino masses

In supergravity GUT models based on  $SU(5)$  gauge symmetry, gaugino masses arise from the Lagrangian term

$$\mathcal{L} \supset \frac{\langle F_\Phi \rangle_{ab}}{M_{Pl}} \lambda_a \lambda_b \quad (2.5)$$

where the  $\lambda_a$  are the gaugino fields, and  $\langle F_\Phi \rangle$  is the vacuum expectation value of the  $F$  term of a chiral superfield which transforms as the symmetric product of two adjoints under  $SU(5)$ :

$$(\mathbf{24} \times \mathbf{24})_{\text{symmetric}} = \mathbf{1} \oplus \mathbf{24} \oplus \mathbf{75} \oplus \mathbf{200}. \quad (2.6)$$

Universal gaugino masses are obtained only if the superfield  $\Phi$  is a singlet of the GUT group. Higher dimensional  $\Phi$  representations yield non-universal gaugino masses at the GUT scale: for the **24**,  $M_1 : M_2 : M_3 = -1 : -3 : 2$ , while for the **75**,  $M_1 : M_2 : M_3 = -5 : 3 : 1$  and for the **200**,  $M_1 : M_2 : M_3 = 10 : 2 : 1$ . Thus, the model parameter space [40] is given by<sup>3</sup>

$$m_0, M_3^0, A_0, \tan\beta \text{ and } \text{sign}(\mu), \quad (2.7)$$

---

<sup>3</sup>Here, we do not consider the possibility that an arbitrary linear combination of these irreducible representations is also possible.

where the  $SU(2)_L$  and  $U(1)_Y$  gaugino masses can be calculated in terms of  $M_3^0$ , the GUT scale  $SU(3)_C$  gaugino mass.

These  $SU(5)$  models with non-universal gaugino masses will yield weak scale gaugino mass values very different from the mSUGRA prediction, and potentially also very different values of the muon anomalous magnetic moment. We have studied the SUSY contributions to  $a_\mu$  within this framework for positive values of  $M_2\mu$ . The  $2\sigma$  region favored by the E821 experiment is shown in the  $m_0$  vs.  $M_3^0$  plane in Fig. 6 for  $\tan\beta = 10$  and Fig. 7 for  $\tan\beta = 35$ . We fix  $A_0 = 0$  in both figures. The frames *a*), *b*) and *c*) respectively show the cases where the superfield  $\Phi$  transforms as a **24**, **75** and **200** dimensional representation of  $SU(5)$ . The corresponding cases for the singlet  $\Phi$  are the mSUGRA cases in Fig. 1*b* and Fig. 1*c*. Again the shaded region in frames *a*) and *c*) is excluded by the same theoretical and experimental constraints discussed for the mSUGRA case. For the **75** case in frame *b*) the theory constraints together with  $m_{\tilde{W}_1} > 100$  GeV exclude the entire plane. However, in the **75** and **200** cases, the mass gap between the chargino and the LSP is very small, and the LEP constraint on the chargino mass may have to be reassessed. In these cases, the lighter neutralinos contain significant higgsino components, and LEP experiments may also be able to probe  $\tilde{Z}_1\tilde{Z}_2$  production as discussed in Ref. [40]. In view of this, in frames *b*), we have chosen to include just the theory constraints in the dark shaded region. In the light shaded region (which covers the rest of the plane in Fig. 7),  $m_{\tilde{W}_1} < 85$  GeV. The various lines labelled by the sparticle type denote contours where  $m_{\tilde{e}_1} = 250$  GeV,  $m_{\tilde{W}_1} = 250$  GeV and  $m_{\tilde{g}} = 1, 2$  TeV. In frames *c*) the selectron is heavier than 250 GeV throughout the allowed region, while the gluino is always lighter than 1 TeV in the allowed range of frame *b*). Finally, the solid lines are contours where  $m_h = 113.5$  GeV, except in frames *b*) where  $h$  is lighter than this throughout: in this case, the solid line labels  $m_h = 110$  GeV.

The area shaded by dots is the region favoured by the E821 experiment at the  $2\sigma$  level. We see that the **24** cases are qualitatively similar to the corresponding mSUGRA cases in Fig. 1, although the allowed region does not extend as far up in the GUT scale gluino mass. The bulk of this region would be accessible at a 500 GeV linear collider for  $\tan\beta \sim 10$ , but even for the larger value of  $\tan\beta$ , a considerable portion of this area will be probed there. While simulations of LHC signals have not been performed within this framework, presumably this entire region will be probed by LHC experiments via the usual multi-jet plus multi-lepton signals. Multi-jet events with identified  $Z$  bosons and  $\cancel{E}_T$  are a characteristic feature of this framework [40].

Moving to the **75** case in frames *b*), we see that the bulk (possibly all) of the parameter plane is already excluded by various constraints already described. Indeed if the region with charginos up to 85 GeV can be excluded either via chargino searches, or via neutralino searches, and  $h$  can definitely be determined to be larger than 110 GeV even after incorporating effects of mixing amongst the CP even scalars, this case will be excluded. In any case, it should be possible to probe this entire region at future colliders, the near degeneracy of the  $\tilde{W}_1$  and  $\tilde{Z}_1$  notwithstanding.

Finally, in frames *c*), we see that the E821 favoured region extends over a large fraction of the plane for both values of  $\tan\beta$ . In the region to the right of the contour labelled  $\tilde{W}_1$ ,  $m_{\tilde{W}_1} < 250$  GeV, and reduces to below the experimental bound as we hit the excluded region. Chargino pair production will thus be accessible only over parts of the parameter space favoured by E821. We have checked that the lighter chargino is higgsino-like, or

for relatively small values of  $M_3^0$  mixed, throughout the plane. Its detection may thus be complicated by the fact that the  $\widetilde{W}_1 - \widetilde{Z}_1$  mass gap is small over much of this range. Again, although explicit LHC simulations have not been performed for this scenario, experiments at the LHC should be sensitive to the SUSY signal over a considerable fraction (if not all) of this parameter range.

To get some flavour of the size of the various contributions to  $a_\mu$ , we present in Table 1 a single case study for each of the models labeled by the dimensionality of the  $\Phi$  representation. The model parameters are also listed in the table. The corresponding sparticle spectrum is listed in Table 4 of Ref. [41]. We recognize that this point may well be excluded by experimental constraints in some of the cases. Our purpose here is only to illustrate how the individual contributions depend on the dimensionality of  $\Phi$ . In the table, we show the magnitude of the various SUSY loop contributions to  $\Delta a_\mu^{SUSY}$ , along with the total. In the case of **1** (universality), we see that the chargino loops dominate, while the  $\widetilde{Z}_2 \widetilde{\mu}_i$  ( $i = 1, 2$ ) loops are also large, but nearly cancel with each other. For this model, the  $\widetilde{Z}_2$  is mainly wino-like. In the **24** model, at the weak scale  $M_1$  decreases by a factor of  $\sim 2$  relative to the mSUGRA case, while  $M_2$  increases by about  $\sim 1.5$ . The loop contributions involving  $\widetilde{W}_i$  decrease relative the mSUGRA case, but still dominate the total contribution. In the **75** model,  $M_2$  increases by about a factor of 3 relative to mSUGRA, while  $M_1$  increases by a factor of about 5. The  $\widetilde{Z}_3$  loops form the dominant neutralino contribution, and the total value of  $\Delta a_\mu^{SUSY}$  is further suppressed. Finally, in the **200** case,  $M_2$  increases by a factor of about 2 at the weak scale relative to mSUGRA, while  $M_1$  increases by about 10. In this case, the  $\widetilde{Z}_4$  is largely wino-like, and it gives the dominant contribution to  $\Delta a_\mu^{SUSY}$ .

### III. GAUGE-MEDIATED SUSY BREAKING MODEL

In recent years, there has been much interest in supersymmetric models where SUSY breaking is communicated via gauge interactions [42]. In these models, SUSY breaking occurs in a hidden sector, but SUSY breaking is communicated from the hidden sector to the observable sector via Standard Model gauge interactions of messenger particles, which are assumed to occur in  $n_5$  complete vector representations of  $SU(5)$  with quantum numbers of  $SU(2)$  doublets of quarks and leptons. The messenger sector mass scale is characterized by  $M$ . The soft SUSY breaking masses for the SUSY partners of SM particles are thus proportional to the strength of their gauge interactions, so that squarks are heavier than sleptons, while the gaugino masses satisfy the usual “grand unification” mass relations, though for very different reasons. Within the minimal version of this framework, the couplings and masses of the sparticles in the observable sector are determined (at the messenger scale  $M$ ) by the parameter set,

$$\Lambda, M, n_5, \tan \beta, \text{sign}(\mu), C_{grav}. \quad (3.1)$$

The parameter  $\Lambda$  sets the scale of sparticle masses and is the most important of these parameters. The model predictions for soft-SUSY breaking parameters at the scale  $M$  are evolved to the weak scale. The parameter  $C_{grav} \geq 1$  and enters only into the partial width for sparticle decays to the gravitino.

In Fig. 8, we show the  $2\sigma$  region favored by the E821 data for the minimal GMSB model. Our plots are in the  $\Lambda$  vs.  $\tan \beta$  plane, for  $M = 3\Lambda$ ,  $\mu > 0$  and a)  $n_5 = 1$ , b)  $n_5 = 2$ , c)

$n_5 = 3$  and  $d)$   $n_5 = 2$  but with  $\mu = 0.75M_1$ . In all cases but  $d)$ , the magnitude of  $\mu$  is fixed by the REWSB constraint. The solid region is excluded either by the REWSB constraint, or by  $m_{\tilde{Z}_1} < 95$  GeV,  $m_{\tilde{e}_1} < 100$  GeV,  $m_{\tilde{\tau}_1} < 76$  GeV or  $m_{\tilde{W}_1} < 100$  GeV, as indicated by LEP2 searches. The solid contour denotes where  $m_h = 113.5$  GeV. Other mass contours listed are  $m_{\tilde{W}_1} = 250$  GeV,  $m_{\tilde{e}_1} = 250$  GeV,  $m_{\tilde{\tau}_1} = 250$  GeV, and  $m_{\tilde{g}} = 1$  and  $2$  TeV (dot-dashed contours). The  $\tilde{W}_1$ ,  $\tilde{e}_1$  and  $\tilde{\tau}_1$  contours correspond to the approximate reach for SUSY particles of a Next Linear Collider operating at  $\sqrt{s} = 500$  GeV. In frame  $a)$ , we see that very little parameter space is favored for low  $\tan\beta$ , but considerable parameter space is favored for large  $\tan\beta$ . The stars correspond to the reach in  $\Lambda$  of the CERN LHC  $pp$  collider for specific GMSB model lines (assuming  $10 \text{ fb}^{-1}$  of integrated luminosity), with the  $\tan\beta$  values sampled in Ref. [43]. The large dots denote the corresponding reach for the Tevatron with  $25 \text{ fb}^{-1}$  of integrated luminosity [44]. In  $a)$ , at least for low  $\tan\beta$ , even the Tevatron reach extends beyond the maximum value of  $\Lambda$  favored by the E821 result, while the reach of the LHC is far beyond. Similar plots are shown in  $b)$  and  $c)$  but for larger numbers of messenger fields. Frame  $d)$  is shown for the special case of a higgsino-like NLSP. For the model lines that have been analyzed [44], we see that for the range of parameters favoured by the E821 data, SUSY signals might well be observable even at the luminosity upgrade of the Tevatron.

#### IV. ANOMALY-MEDIATED SUSY BREAKING MODEL

It has recently been recognized [45] that there exist loop contributions to sparticle masses originating in the super-Weyl anomaly, which is always present in supergravity models when SUSY is broken. In models without SM gauge singlet superfields that can acquire a Planck scale vev, the usual supergravity contribution to gaugino masses is suppressed by an additional factor  $\frac{M_{SUSY}}{M_P}$  relative to  $m_{\frac{3}{2}} = M_{SUSY}^2/M_P$ , or in higher dimensional models where the coupling between the observable and hidden sectors is strongly suppressed, these anomaly-mediated contribution can dominate. The gaugino masses turn out to be non-universal, and are found to be proportional to the respective gauge group  $\beta$ -functions. Likewise, scalar masses and trilinear terms are given in terms of gauge group and Yukawa interaction beta functions. Slepton squared masses turn out to be negative (tachyonic). A common fix is to assume an additional contribution  $m_0^2$  for all scalars. The parameter space of the model then consists of

$$m_0, m_{3/2}, \tan\beta \text{ and } \text{sign}(\mu). \quad (4.1)$$

In the minimal AMSB model (mAMSB), the  $\tilde{W}_1$  and  $\tilde{Z}_1$  are both wino-like, and nearly mass degenerate, leading to a unique phenomenology [46].

In Fig. 9, we show plots of the mAMSB parameter space via the  $m_0$  vs.  $m_{3/2}$  plane, for  $\mu < 0$ , and for  $a)$   $\tan\beta = 3$ ,  $b)$   $\tan\beta = 10$  and  $c)$   $\tan\beta = 35$ . For AMSB models,  $\mu < 0$  yields  $\Delta a_\mu^{SUSY} > 0$ , since we take the gaugino masses  $M_1$  and  $M_2$  to be negative in ISAJET.<sup>4</sup> Incidentally, this sign of  $\mu$  appears to be disfavoured by constraints on  $BR(b \rightarrow s\gamma)$

---

<sup>4</sup>We have corrected an error in the sign of the  $A$ -parameters that was present in ISAJET v7.51.

as obtained in Ref. [47]. The solid regions are excluded by lack of the correct pattern of REWSB, or when  $\tilde{\tau}_1$  is the LSP, or by  $m_{\tilde{W}_1} < 86$  GeV (from LEP2 chargino searches in the mAMSB model [48]). In frame *a*), only a tiny region at the lower left is within the  $2\sigma$  range of  $\Delta a_\mu$  as measured by E821. Moreover, in this entire plane  $m_h < 113.5$  GeV. The solid contour denotes where  $m_h = 105$  GeV: thus, even allowing for effects of mixing in the Higgs sector, much of this plane is presumably excluded. The dashed-dotted contour denotes the reach of the CERN LHC for mAMSB models with  $10 \text{ fb}^{-1}$  of integrated luminosity [49]. In frame *b*), the solid contour denotes where  $m_h = 113.5$  GeV, and the dotted shading denotes the  $2\sigma$  favored region of  $\Delta a_\mu^{SUSY}$ . Only a small region has  $\Delta a_\mu^{SUSY} > 10 \times 11^{-10}$ , and  $m_h > 113.5$  GeV. We do not show any dashed-dotted contour as there was no computation of the LHC reach for this value of  $\tan \beta$ . In *c*), for  $\tan \beta = 35$ , we find that a considerable region of parameter space is favored by the muon anomalous moment, while simultaneously having  $m_h > 113.5$  GeV (solid contour). The reach of CERN LHC encompasses almost the entire favored region.

## V. GAUGINO-MEDIATED SUSY BREAKING MODEL

A fourth class of models has been recently proposed, based on extra dimensions with branes, which provides a novel solution to the SUSY flavor and  $CP$  problems [50]. In this framework, chiral supermultiplets of the observable sector reside on one brane whereas the SUSY breaking sector is confined to a different brane. Gravity and gauge superfields propagate in the bulk, and hence, directly couple to fields on both the branes. As a result of their direct coupling to the SUSY breaking sector, gauginos acquire a mass. The scalar components of the chiral supermultiplets, however, can acquire a SUSY breaking mass only via their interactions with gauginos (or gravity) which feel the effects of SUSY breaking: as a result, these masses are suppressed relative to gaugino masses, and may be neglected in the first approximation. The same is true for the  $A$  parameters.

To gain a phenomenologically acceptable sparticle mass spectrum, it is necessary to include additional renormalization group running between the assumed compactification scale  $M_c$  and  $M_{GUT}$ . At energies above  $M_{GUT}$ , it is assumed that either  $SO(10)$  or  $SU(5)$  grand unification is valid. Thus, all scalars have masses  $m_0 = 0$  at  $M_c$ , but non-zero values at  $M_{GUT}$ . The parameter space of the model consists of [41]

$$m_{1/2}, M_c, \tan \beta, \text{sign}(\mu). \quad (5.1)$$

If one insists on a high degree of Yukawa coupling unification, then one is forced to require  $\mu < 0$ . In this case,  $\Delta a_\mu^{SUSY}$  will always be negative. Yukawa coupling unification also highly restricts the allowed values of  $\tan \beta$ . Other parameters may be necessary in addition to the above set depending on the specific model of grand unification assumed.

In Fig. 10, we assume the inoMSB boundary conditions to be valid at  $M_c = 1 \times 10^{18}$  GeV, and that minimal  $SU(5)$  grand unification is valid between  $M_c$  and  $M_{GUT} \simeq 2 \times 10^{16}$  GeV. We use the  $SU(5)$  RGEs given in Ref. [41], with Yukawa couplings  $f_t = 0.519$ , and

---

This does not affect the results in Ref. [49].

$f_b = f_\tau = 0.277$  at  $M_{GUT}$ , which are characteristic of  $\tan\beta = 35$ . Two additional  $SU(5)$  Yukawa couplings  $\lambda = 1$  and  $\lambda' = 0.1$  are assumed. Several representative sparticle masses are shown in frame *a*), along with the value of  $|\mu|$ . Note that the lower bound on parameter space of  $m_{1/2} \simeq 280$  GeV occurs where  $m_{\tilde{\tau}_1} = m_{\tilde{Z}_1}$ . In frame *b*), we show the corresponding value of  $\Delta a_\mu^{SUSY}$ . As expected, it is always negative. However, for  $m_{1/2} > 1$  TeV, it lies within the  $3\sigma$  bound from E821. In this case, the model is moving towards the region of unnaturality.

## VI. SUMMARY AND CONCLUSIONS

The recently reported measurement of  $a_\mu$  by the Muon ( $g-2$ ) Experiment E821 has been interpreted as a harbinger of physics beyond the Standard Model. This will be so if in fact the quoted SM estimate of  $a_\mu$  and its associated error are verified, and if the experimental measurement is maintained with a reduced error after the analysis of the year 2000 data. If the discrepancy between the measured and theoretical values of  $a_\mu$  persists, then the result will act as a strong constraint on many forms of new physics, including weak scale supersymmetric matter.

We presented here the values of  $\Delta a_\mu^{SUSY}$  expected in a variety of supersymmetric models. The quoted discrepancy [1] between theory and experiment can easily be accommodated in a variety of supersymmetric models. Models with a negative value of  $\mu M_2$  or TeV scale scalars, however, are disfavored. The former include models that incorporate a high degree of Yukawa coupling unification, while the latter include models that invoke a decoupling solution to the SUSY flavor and CP problems. Amongst these are focus point models at intermediate (but not high)  $\tan\beta$ , and models with an inverted scalar mass hierarchy. Even so, like the SM, these decoupling models are generally allowed at the  $3\sigma$  level.

## ACKNOWLEDGMENTS

We thank F. Paige and J. Feng for discussions and comments. This research was supported in part by the U. S. Department of Energy under contract numbers DE-FG02-97ER41022 and DE-FG03-94ER40833. J. Ferrandis was supported by a spanish MEC-FPI grant and by the European Commission TMR contract HPRN-CT-2000-00148.

## REFERENCES

- [1] H. N. Brown *et al.* (Muon  $g - 2$  Collaboration), Phys. Rev. Lett. **86**, 2227 (2001).
- [2] A. Czarnecki and W. Marciano, hep-ph/0102122 (2001).
- [3] M. Davier and A. Höcker, Phys. Lett. **B435**, 427 (1998).
- [4] F. J. Yndurain, hep-ph/0102312 (2001).
- [5] J. Lopez, D. Nanopoulos and X. Wang, Phys. Rev. **D49**, 366 (1994); U. Chattopadhyay and P. Nath, Phys. Rev. **D53**, 1648 (1996); M. Carena, G. Giudice and C. Wagner, Phys. Lett. **B390**, 234 (1997); U. Chattopadhyay, D.K. Ghosh and S. Roy, Phys. Rev. **D62**, 115001 (2000).
- [6] T. Moroi, Phys. Rev. **D53**, 6565 (1996).
- [7] L. Everett, G. Kane, S. Rigolin and L. Wang, hep-ph/0102145 (2001).
- [8] J. Feng and K. Matchev, hep-ph/0102146 (2001).
- [9] E. Baltz and P. Gondolo, hep-ph/0102147 (2001).
- [10] U. Chattopadhyay and P. Nath, hep-ph/0102157 (2001).
- [11] S. Komine, T. Moroi and M. Yamaguchi, hep-ph/0102204 (2001).
- [12] J. Hisano and K. Tobe, hep-ph/0102315 (2001).
- [13] J. Ellis, D. Nanopoulos and K. Olive, hep-ph/0102331 (2001).
- [14] R. Arnowitt, B. Dutta, B. Hu and Y. Santoso, hep-ph/0102344 (2001).
- [15] M. Einhorn and J. Wudka, hep-ph/0103034 (2001).
- [16] K. Choi, K. Hwang, S. Kang, K. Lee and W. Song, hep-ph/0103048 (2001).
- [17] J. E. Kim, B. Kyae and H. M. Lee, hep-ph/0103054 (2001).
- [18] S. Martin and J. D. Wells, hep-ph/0103067 (2001).
- [19] See also T. Blazek, hep-ph/9912460 (1999).
- [20] A. Chamseddine, R. Arnowitt and P. Nath, Phys. Rev. Lett. **49**, 970 (1982); R. Barbieri, S. Ferrara and C. Savoy, Phys. Lett. **B119**, 343 (1982); L.J. Hall, J. Lykken and S. Weinberg, Phys. Rev. **D27**, 2359 (1983); for a review, see H. P. Nilles, Phys. Rep. **110**, 1 (1984).
- [21] F. Paige, S. Protopopescu, H. Baer and X. Tata, hep-ph/0001086 (2000).
- [22] P. Igo-Kemenes, *presented at the Int. Conf. on High Energy Physics*, Osaka, Japan, (July, 2000).
- [23] H. Baer, M. Drees, F. Paige, P. Quintana and X. Tata, Phys. Rev. **D61**, 095007 (2000); V. Barger and C. Kao, Phys. Rev. **D60**, 115015 (1999); K. Matchev and D. Pierce, Phys. Lett. **B467**, 225 (1999).
- [24] S. Abel *et al.* (SUGRA Working Group Collaboration), hep-ph/0003154 (2000).
- [25] H. Baer, C. H. Chen, F. Paige and X. Tata, Phys. Rev. **D52**, 2746 (1995) and Phys. Rev. **D53**, 6241 (1996); H. Baer, C. H. Chen, M. Drees, F. Paige and X. Tata, Phys. Rev. **D59**, 055014 (1999).
- [26] J. Feng, K. Matchev and T. Moroi, Phys. Rev. Lett. **84**, 2322 (2000) and Phys. Rev. **D61**, 075005 (2000).
- [27] See *e.g.* H. Baer and M. Brhlik, Phys. Rev. **D55**, 3201 (1997); H. Baer, M. Brhlik, D. Castano and X. Tata, Phys. Rev. **D58**, 015007 (1998).
- [28] H. Baer and M. Brhlik, Phys. Rev. **D53**, 597 (1996) and Phys. Rev. **D57**, 567 (1998); V. Barger and C. Kao, Phys. Rev. **D57**, 3131 (1998).
- [29] J. Feng, K. Matchev and F. Wilczek, Phys. Lett. **B482**, 388 (2000).
- [30] J. Ellis, T. Falk, G. Gani, K. Olive and M. Srednicki, hep-ph/0102098 (2001).

- [31] Y. Fukuda *et al.*, Phys. Rev. Lett. **82**, 2644 (1999) and Phys. Rev. Lett. **85**, 3999 (2000).
- [32] See *e.g.* T. Blazek, S. Raby and K. Tobe, Phys. Rev. **D60**, 113001 (1999); C. Aulakh, A. Melfo, A. Rasin and G. Senjanovic, Phys. Lett. **B459**, 557 (1999); K. S. Babu, J. Pati and F. Wilczek, Nucl. Phys. **B566**, 33 (2000); C. Albright and S. M. Barr, Phys. Rev. **D62**, 093008 (2000); for a review, see R. Mohapatra, hep-ph/9911272 (1999).
- [33] H. Baer, M. Diaz, J. Ferrandis and X. Tata, Phys. Rev. **D61**, 111701 (2000); H. Baer, M. Brhlik, M. Diaz, J. Ferrandis, P. Mercadante, P. Quintana and X. Tata, Phys. Rev. **D63**, 015007 (2001).
- [34] F. Gabbiani, E. Gabrielli, A. Masiero and L. Silvestrini, Nucl. Phys. **B477**, 321 (1996).
- [35] J. Feng, C. Kolda and N. Polonsky, Nucl. Phys. **B546**, 3 (1999); J. Bagger, J. Feng and N. Polonsky, Nucl. Phys. **B563**, 3 (1999); J. Bagger, J. Feng, N. Polonsky and R. Zhang, Phys. Lett. **B473**, 264 (2000).
- [36] H. Baer, P. Mercadante and X. Tata, Phys. Lett. **B475**, 289 (2000).
- [37] H. Baer, C. Balázs, M. Brhlik, P. Mercadante, X. Tata and Y. Wang, hep-ph/0102156 (2001), Phys. Rev. D (in press).
- [38] N. Arkani-Hamed and H. Murayama, Phys. Rev. **D56**, R6733 (1997); K. Agashe and M. Graesser, Phys. Rev. **D59**, 015007 (1999).
- [39] H. Baer, C. Balázs, P. Mercadante, X. Tata and Y. Wang, Phys. Rev. **D63**, 015011 (2001).
- [40] G. Anderson, H. Baer, C. Chen, P. Quintana and X. Tata, Phys. Rev. **D61**, 095005 (2000).
- [41] H. Baer, M. Diaz, P. Quintana and X. Tata, JHEP **4**, 016 (2000).
- [42] M. Dine and A. Nelson, Phys. Rev. **D48**, 1277 (1993); M. Dine, A. Nelson, Y. Shirman, Phys. Rev. **D51**, 1362 (1995); M. Dine, A. Nelson, Y. Nir and Y. Shirman, Phys. Rev. **D53**, 2658 (1996); for a review, see G. Giudice and R. Rattazzi, Phys. Rep. **322**, 419 (1999).
- [43] H. Baer, P. Mercadante, X. Tata and Y. Wang, Phys. Rev. **D62**, 095007 (2000).
- [44] H. Baer, P. Mercadante, X. Tata and Y. Wang, Phys. Rev. **D60**, 055001 (1999); the reach in frame  $d$ ) was obtained by Y. Wang, Ph. D thesis (in preparation), assuming that the background in the inclusive  $Z\gamma + \cancel{E}_T$  channel is negligible.
- [45] L. Randall and R. Sundrum, Nucl. Phys. **B557**, 79 (1999); G. Giudice, M. Luty, H. Murayama and R. Rattazzi, JHEP **9812**, 027 (1998).
- [46] J. Feng and T. Moroi, Phys. Rev. **D61**, 095004 (2000); T. Gherghetta, G. Giudice and J. Wells, Nucl. Phys. **B559**, 27 (1999).
- [47] J. Feng and T. Moroi, Ref. [46].
- [48] G. Grenier, talk given at SUSY2K meeting, Cern, Geneva, June, 2000.
- [49] H. Baer, K. Mizukoshi and X. Tata, Phys. Lett. **B488**, 367 (2000).
- [50] M. Schmaltz and W. Skiba, Phys. Rev. **D62**, 095004 (2000) and *ibid* **D62**, 095005 (2000).

## TABLES

TABLE I. Loop contributions to  $\Delta a_\mu^{SU5}$  in  $SU(5)$  models with non-universal gaugino masses. Each contribution must be multiplied by  $10^{-10}$ . We adopt the parameter space point  $(m_0, M_3^0, A_0) = (100, 150, 0)$  GeV, with  $\tan\beta = 5$ . For each case,  $\mu > 0$  except model **24**, for which  $\mu < 0$ .

| loop                                  | <b>1</b> | <b>24</b> | <b>75</b> | <b>200</b> |
|---------------------------------------|----------|-----------|-----------|------------|
| $\widetilde{W}_1 \widetilde{\nu}_\mu$ | 44.5     | 38.1      | 11.6      | 19.4       |
| $\widetilde{W}_2 \widetilde{\nu}_\mu$ | -11.8    | -15.6     | -3.62     | -10.5      |
| $\widetilde{Z}_1 \widetilde{\mu}_1$   | 4.58     | -1.57     | 0.55      | -2.84      |
| $\widetilde{Z}_2 \widetilde{\mu}_1$   | 21.2     | 8.01      | 0.71      | 0.06       |
| $\widetilde{Z}_3 \widetilde{\mu}_1$   | -1.15    | -2.08     | -2.47     | 5.49       |
| $\widetilde{Z}_4 \widetilde{\mu}_1$   | -0.25    | 0.07      | -0.04     | 48.5       |
| $\widetilde{Z}_1 \widetilde{\mu}_2$   | -7.56    | -1.32     | -1.31     | 0.05       |
| $\widetilde{Z}_2 \widetilde{\mu}_2$   | -21.8    | -9.74     | -0.69     | -0.37      |
| $\widetilde{Z}_3 \widetilde{\mu}_2$   | -1.49    | -0.77     | 1.84      | -1.75      |
| $\widetilde{Z}_4 \widetilde{\mu}_2$   | 6.14     | 5.37      | 0.96      | -33.3      |
| <i>total</i>                          | 32.4     | 20.4      | 7.53      | 24.7       |



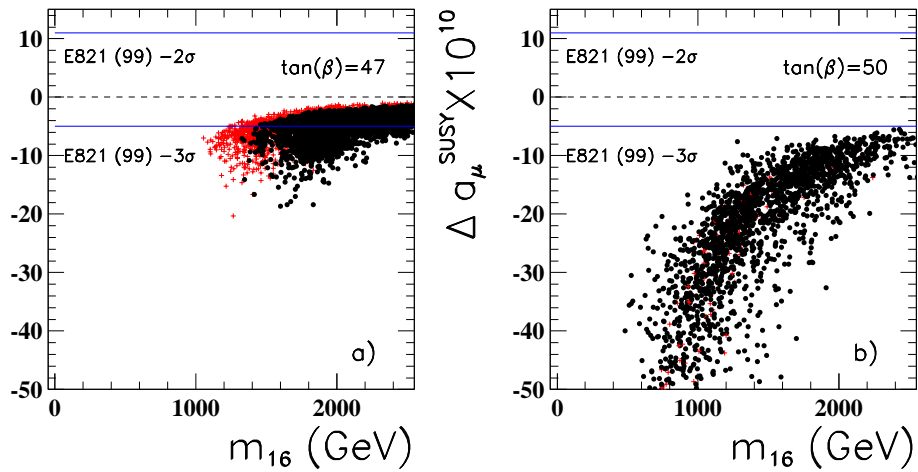


FIG. 2. A plot of the  $\Delta a_\mu^{SUSY}$  value for various Yukawa unified  $SO(10)$  models with *a)*  $\tan \beta = 47$ , and  $\mu < 0$  and *b)*  $\tan \beta = 50$  and  $\mu < 0$ . We require  $t - b - \tau$  Yukawa unification at  $M_{GUT}$  at the 5% level. The pluses are valid solutions but have some sparticle or Higgs masses in conflict with LEP2 constraints.

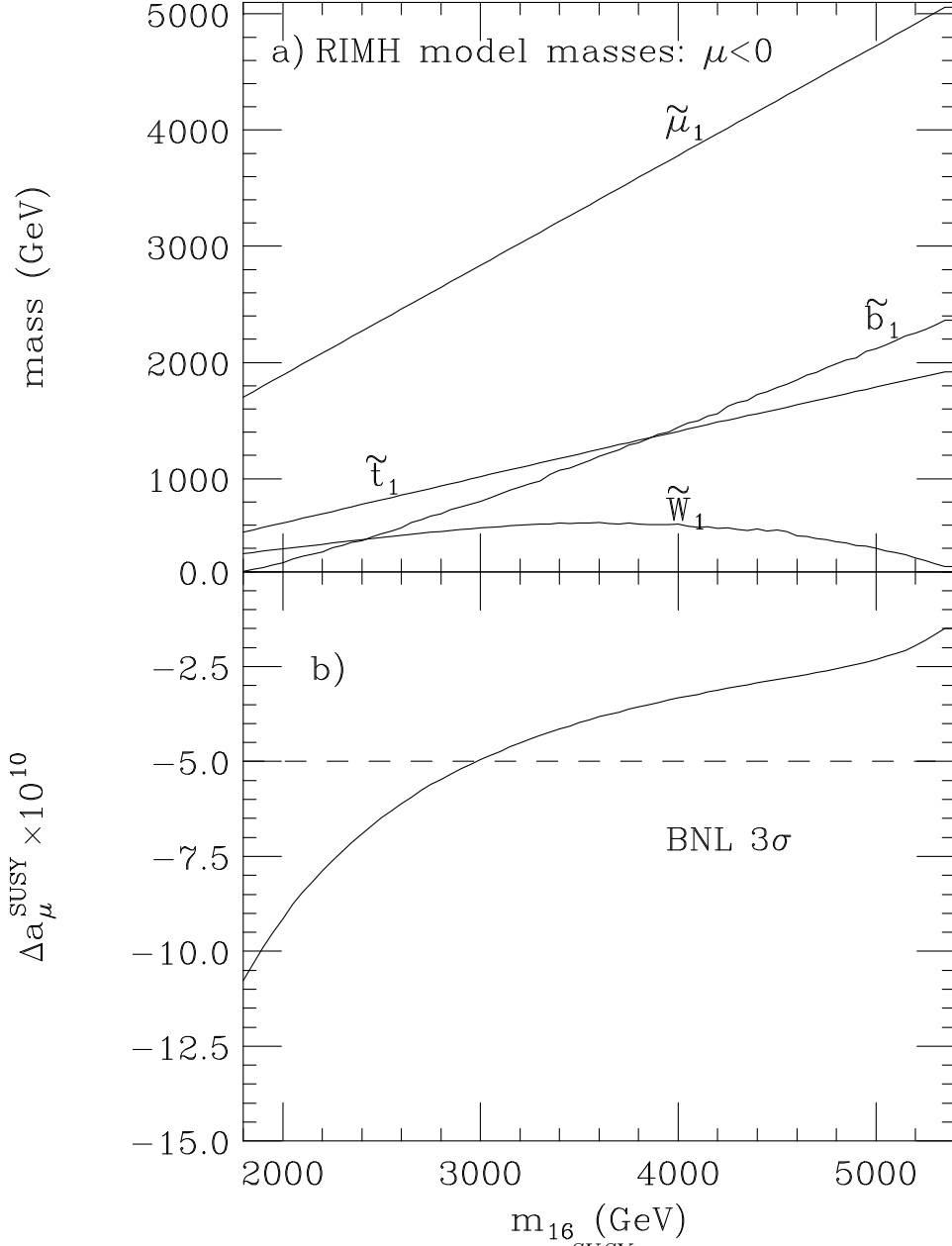


FIG. 3. A plot of a) sparticle masses and b)  $\Delta a_\mu^{\text{SUSY}}$  versus  $m_{16}$  for RIMH models with  $m_{1/2} = 0.25m_{16}$ ,  $M_D = 0.2m_{16}$ ,  $\tan\beta = 50$ ,  $\mu < 0$  and  $M_N = 1 \times 10^7$  GeV.

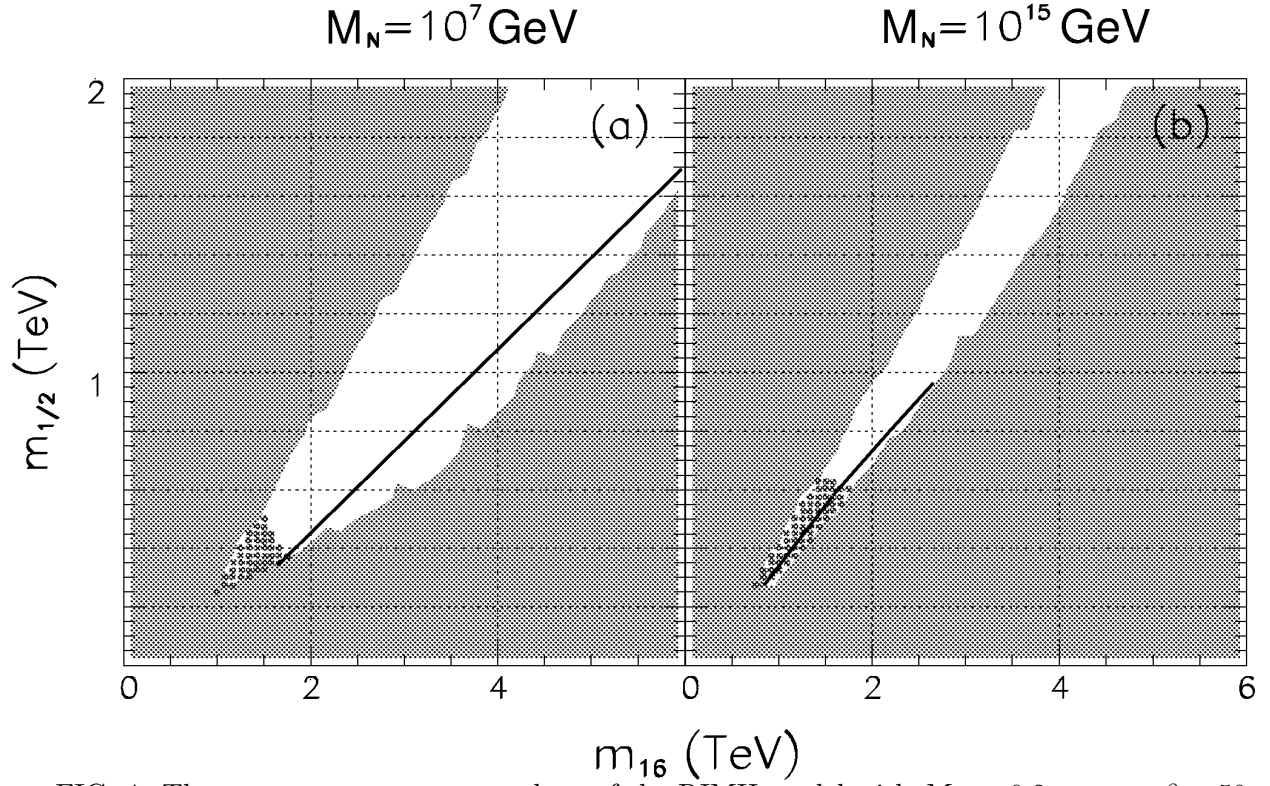


FIG. 4. The  $m_{16} - m_{1/2}$  parameter plane of the RIMH model with  $M_D = 0.2m_{16}$ ,  $\tan\beta = 50$ ,  $\mu > 0$ , and a)  $M_N = 1 \times 10^7 \text{ GeV}$  and b)  $M_N = 10^{15} \text{ GeV}$ . The shaded region is excluded by the theoretical constraints discussed in the text. To the right of the solid line, the crunch factor  $S > 4$ . In the region shaded with dots, the SUSY contribution to  $a_\mu$  is within  $2\sigma$  of the central value obtained by the E821 experiment.

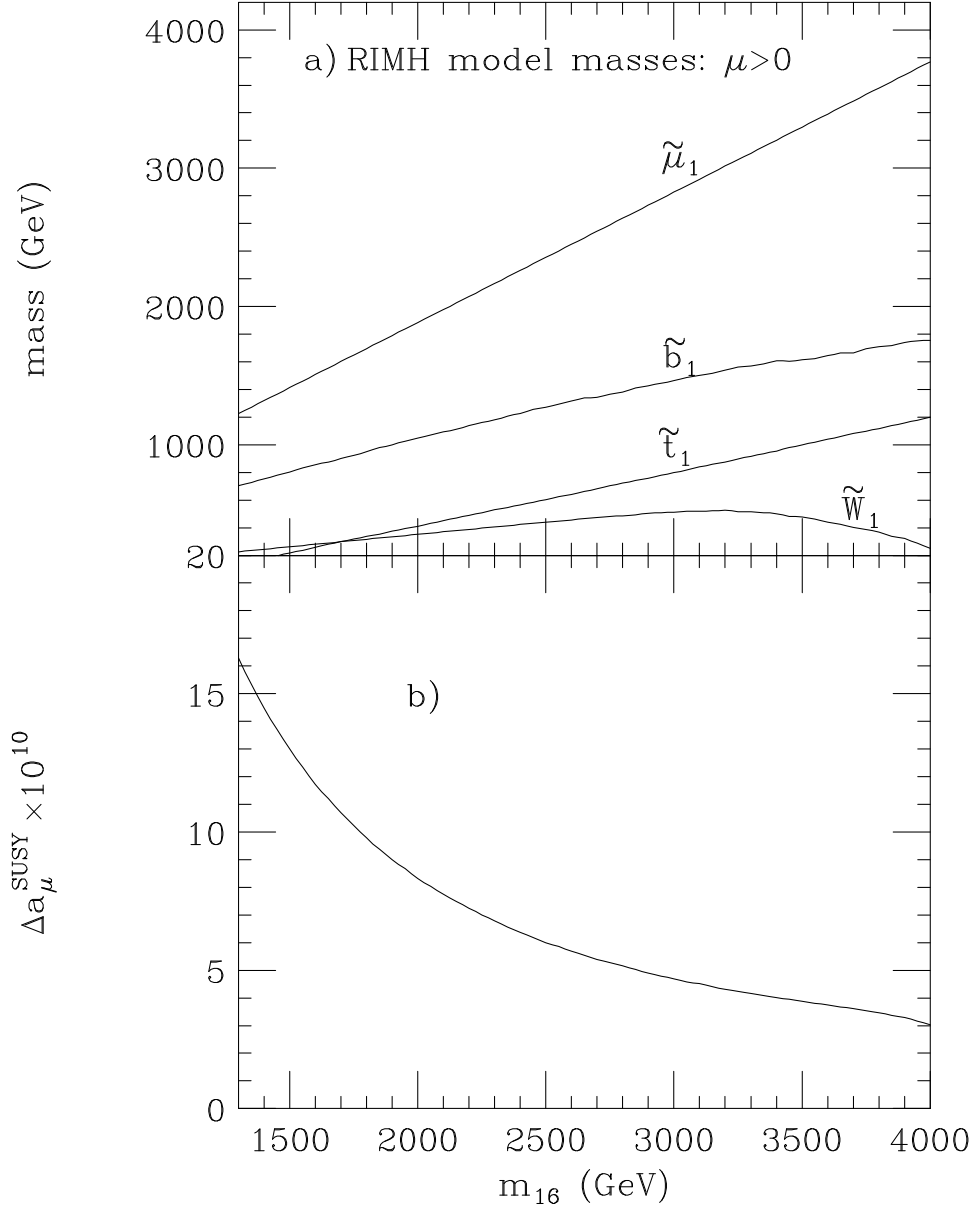


FIG. 5. A plot of *a*) sparticle masses and *b*)  $\Delta a_{\mu}^{\text{SUSY}}$  versus  $m_{16}$  for RIMH models with  $m_{1/2} = 0.22m_{16}$ ,  $M_D = 0.2m_{16}$ ,  $\tan \beta = 50$ ,  $\mu > 0$  and  $M_N = 1 \times 10^7$  GeV.

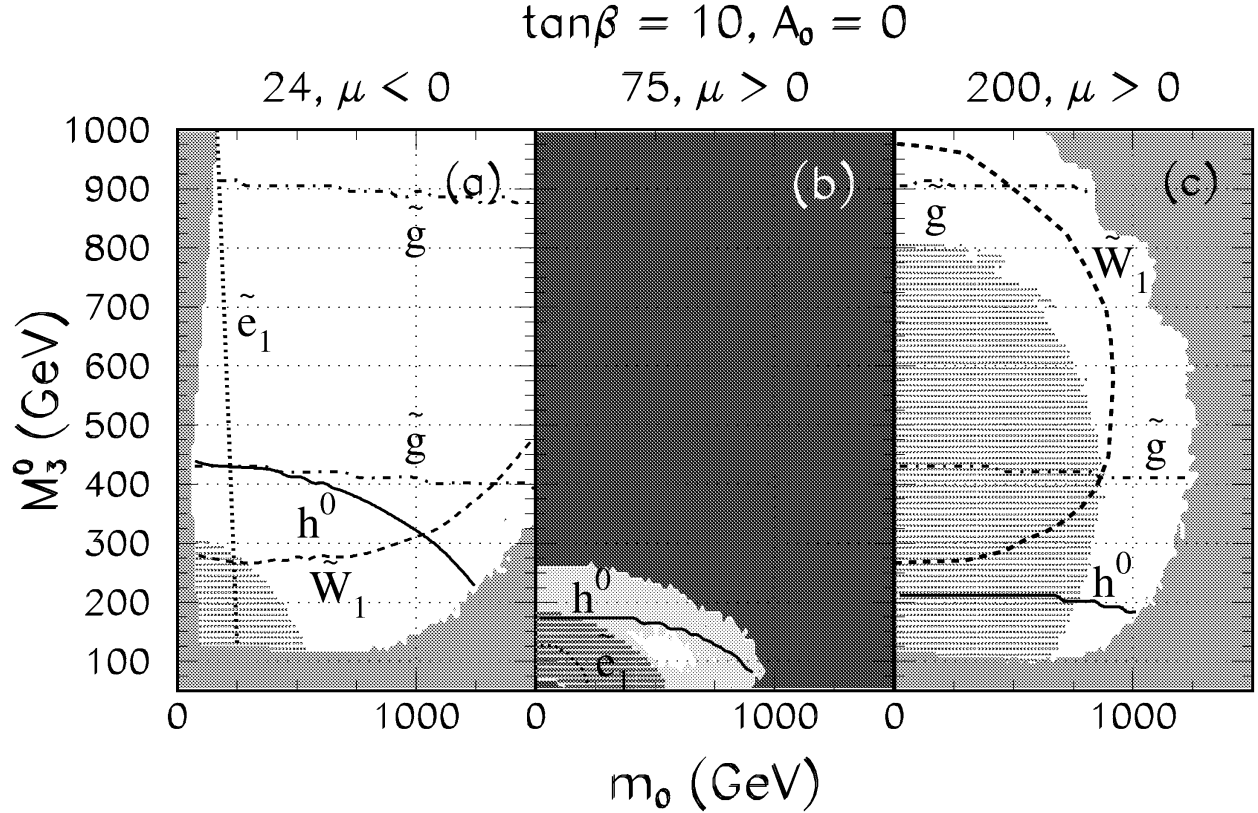


FIG. 6. A plot of the  $m_0$  vs.  $M_3^0$  parameter plane of the  $SU(5)$  model with non-universal gaugino masses discussed in Sec. IID for the case where the superfield  $\Phi$  transforms as a *a)* **24**, *b)* **75**, and *c)* **200** dimensional representation of  $SU(5)$ . We have fixed  $A_0 = 0$  and  $\tan\beta = 10$ . The shaded region in frames *a)* and *c)* is excluded by experimental and theoretical constraints discussed in the text. In frame *b)*, however, the dark shaded region corresponds to just the theoretical constraints, while in the light shaded region  $m_{\tilde{W}_1} < 85$  GeV. In the white region around  $m_0 \sim 500$  GeV and  $M_3^0 = 125$  GeV, the chargino is between 85 and 100 GeV. The various lines labelled by a particle type are contours of sparticle masses as discussed in the text. Finally, the  $2\sigma$  region favoured by the E821 experiment is shaded with dots.

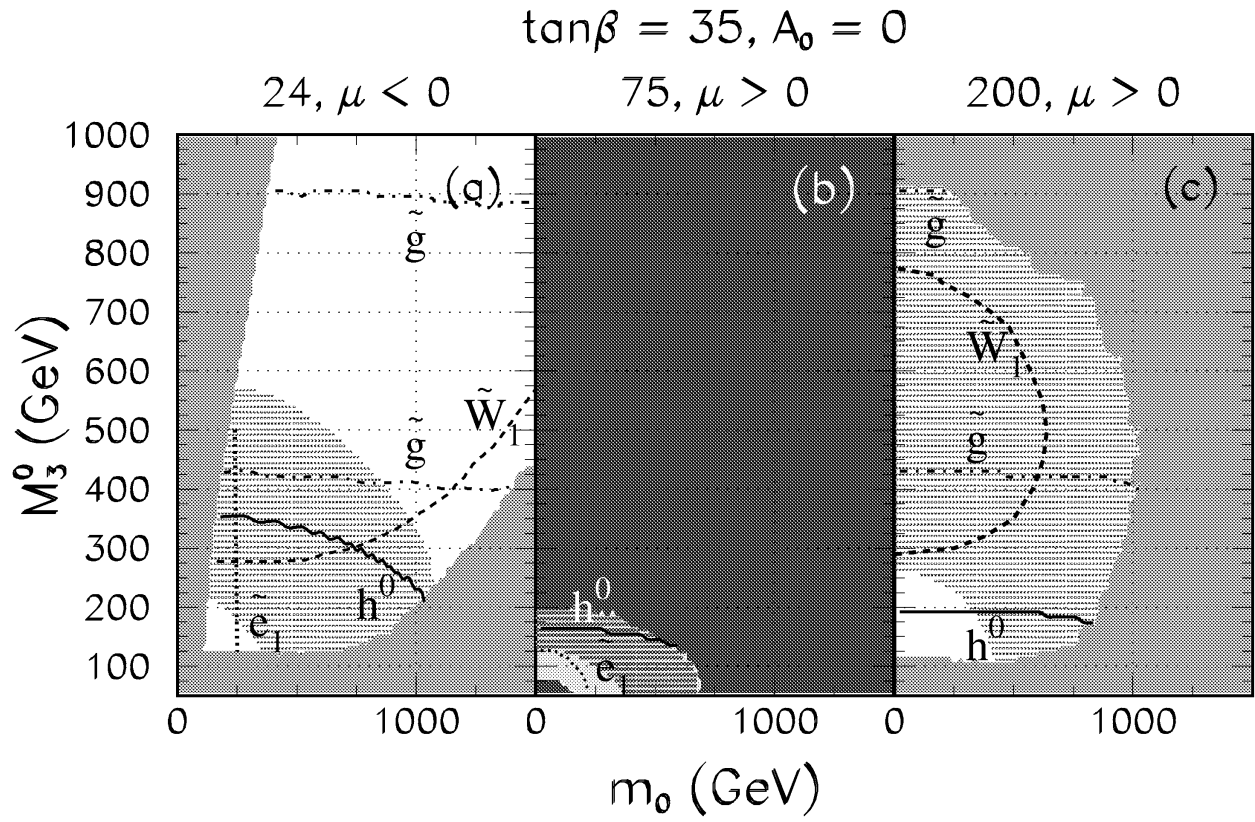


FIG. 7. The same as Fig. 6 except that  $\tan\beta = 35$ .

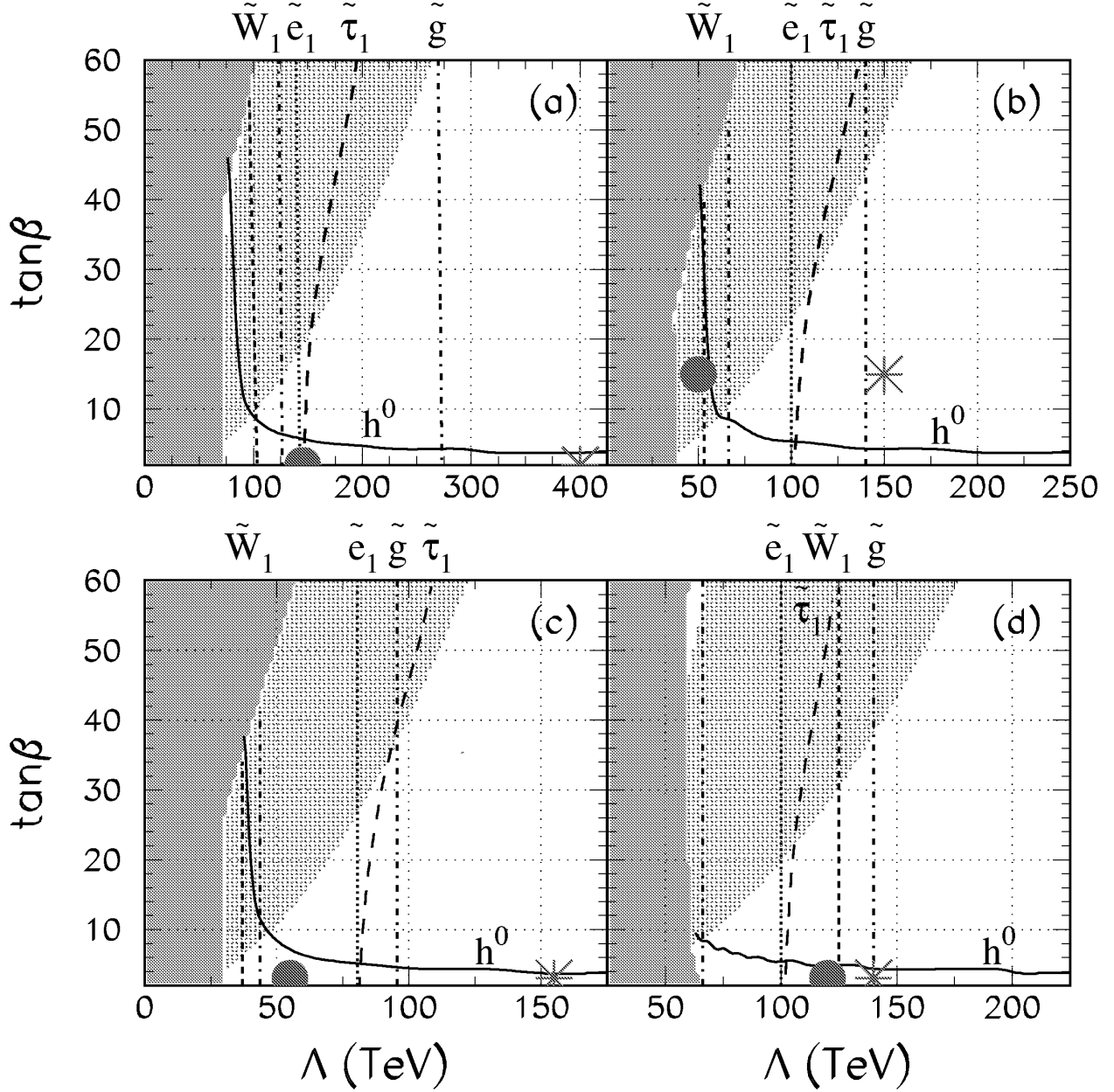


FIG. 8. A plot of parameter space in the minimal GMSB model, for  $M = 3\Lambda$ , and  $\mu > 0$ . In *a*), we take  $n_5 = 1$ , in *b*),  $n_5 = 2$ , in *c*)  $n_5 = 3$  and in *d*),  $n_5 = 2$  but with  $\mu = 0.75M_1$ . The  $2\sigma$  region favored by E821 is shaded with dots. The reach in  $\Lambda$  of the CERN LHC for particular model lines with specific  $\tan\beta$  values is indicated by asterisks. For instance, in frame *a*) the model line studied had  $\tan\beta = 2$  and the reach extending to  $\Lambda$  beyond 400 TeV. The large dots denote the corresponding reach of a luminosity upgrade of the Tevatron that yields  $25 fb^{-1}$  of integrated luminosity.

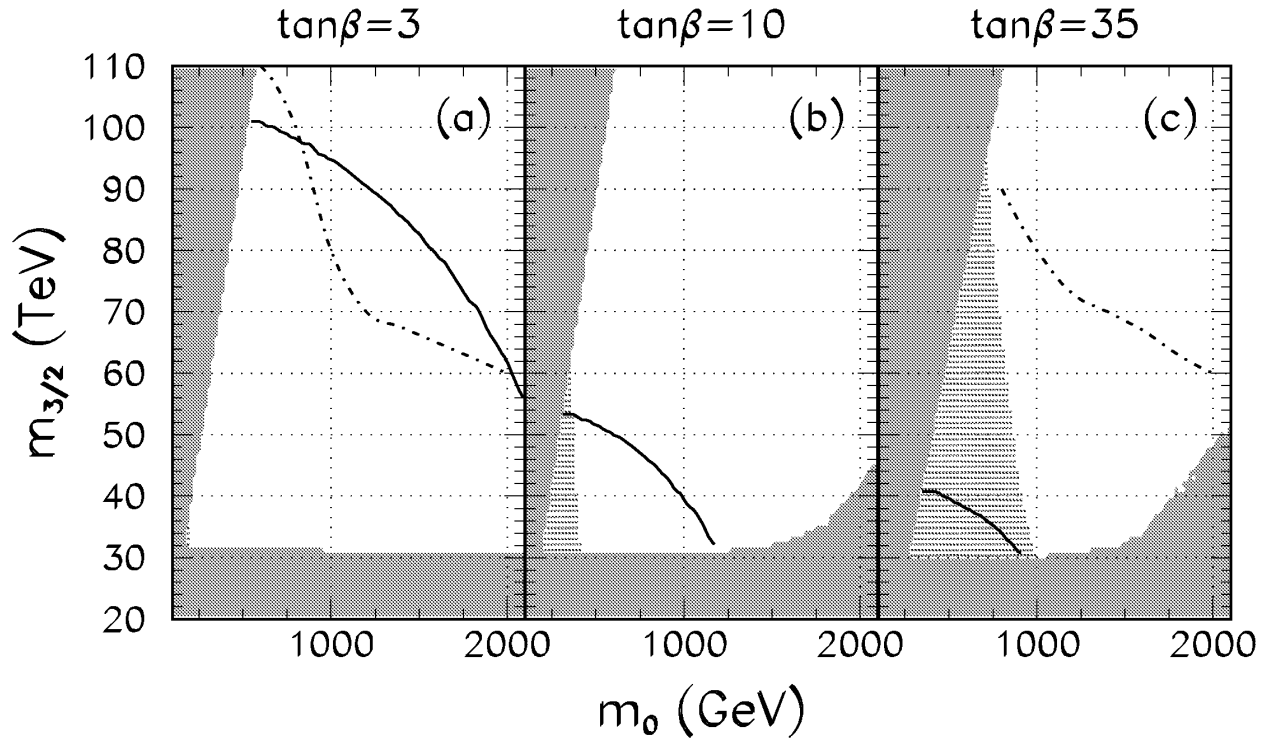


FIG. 9. A plot of parameter space in the minimal AMSB model, for  $\mu < 0$  and *a*)  $\tan\beta = 3$ , *b*)  $\tan\beta = 10$  and *c*)  $\tan\beta = 35$ . In *a*), the solid contour denotes where  $m_h = 105$  GeV, while in *b*) and *c*) it denotes where  $m_h = 113.5$  GeV. The  $2\sigma$  region favored by E821 is shaded with dots. The dot-dashed contours denote the boundary of the region that will be probed by the CERN LHC with  $10 \text{ fb}^{-1}$  of integrated luminosity.

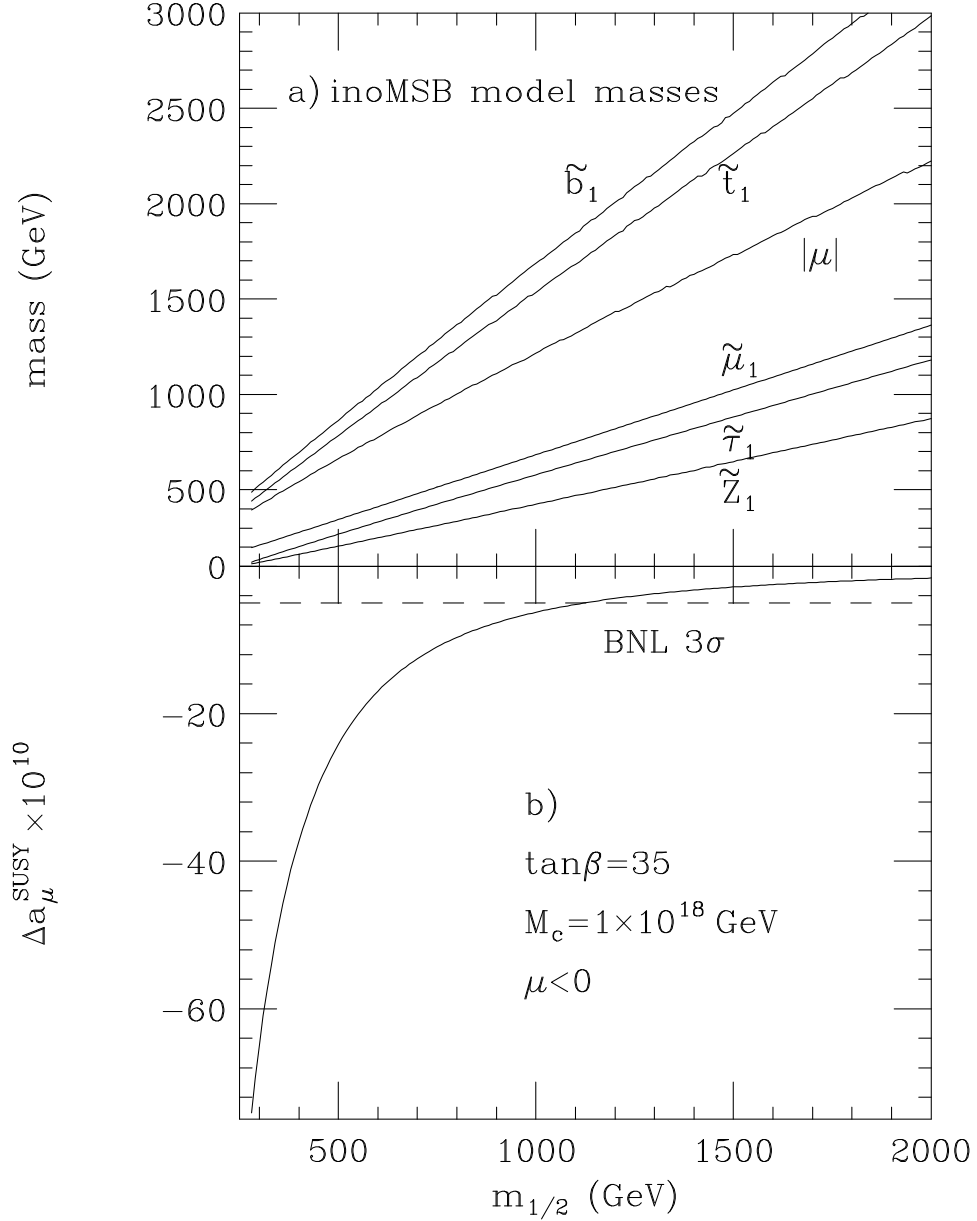


FIG. 10. A plot of a) sparticle masses and b)  $\Delta a_\mu^{SUSY}$  versus  $m_{1/2}$  in the minimal gaugino-mediated SUSY breaking model, for  $\tan\beta = 35$ , and  $\mu < 0$ . We assume  $SU(5)$  unification between  $M_c$  and  $M_{GUT}$ .